Nucleon-nucleon final-state interactions in NN → NNπ

J. Dubach

*Department of Physics and Astronomy, University of Massachusetts,
Amherst, Massachusetts 01003*

W. M. Kloet

Department of Physics and Astronomy, Rutgers University, New Brunswick, New Jersey 08903

R. R. Silbar

*Theoretical Division, University of California, Los Alamos National Laboratory,
Los Alamos, New Mexico 87545*

Peaks in cross sections for the NN → NNπ reaction at low relative momentum for the final nucleon-nucleon pair are successfully explained using $^1S_0$ and $^3S_1$ final-state interactions. Both singlet and triplet final-state interactions are important and can interfere dramatically in certain spin observables.

It has become abundantly clear in the last few years that a prominent experimental feature in the reaction NN → NNπ at intermediate energies is the final-state interaction (FSI) of the two outgoing nucleons.[1-4] This can be seen as peaks in the spin-averaged differential cross sections for those kinematic conditions which allow small relative momenta in the final-state NN pair.[1] To a lesser extent these effects can also be seen in the spin observables, such as polarization asymmetries.[3]

Most theoretical calculations for the NN → NNπ reaction have not attempted to include the FSI effect. One notable exception is the peripheral model work by VerWest.[5] For spin-averaged cross sections VerWest's predictions are reasonably successful. However, such an approach, which is essentially a Born approximation calculation, cannot be expected to give detailed information on relative phases, such as are measured in a polarization experiment.

In this paper we extend our unitary, unified model of NN and NNπ interactions[6] to include FSI corrections. The approach follows the spirit of the Watson-Migdal final-state interaction prescription, in which our model T matrix for a particular NN → NNπ reaction is multiplied by a factor which incorporates the FSI between the final nucleons in relative s waves. (Our three-body model has, at this stage, two-body pion-nucleon input interactions, but no "direct" two-body NN interactions.) In detail, as discussed below, we follow closely the discussion given in the scattering theory text by Taylor.[7]

It is useful to remember that the nucleon-nucleon FSI effects involve only a very restricted range of the available three-body final-state phase space. Here we consider FSI for both $^1S_0$ and $^3S_1$ NN states. Generally, the $^1S_0$ FSI is dominant in nuclear reactions. However, the $^1S_0$ final NN state is suppressed in the NN → NNπ reaction because of selection rules, and we find it is necessary to include the $^3S_1$ FSI as well. In fact, the triplet FSI is often the most important effect. We note in passing that, for essentially the same reasons, the absorption of pions on $^1S_0$ NN pairs in nuclei is also suppressed, relative to $^3S_1$ absorption.[8]

After a discussion of how we include the FSI factor, a sampling of our computational results is given for spin-averaged differential cross sections for pion production.

Our relatively crude approach does surprisingly well in reproducing the general features of the FSI effects seen in the data. (Were one to include direct NN two-body interactions as input in the three-body calculations, the computational complexities would be increased considerably.) We then also present calculations of spin observables for the NN → NNπ reaction. One surprising result is that while the spin-averaged differential cross section often shows dramatic effects due to the FSI, the effects on spin observables are generally small. Often they are even negligible. This seems to agree with the general experimental situation. For example, the extensive measurements by Hollas *et al.*[4] show the FSI peak in some cross sections very clearly, but quantities such as the spin transfer D_{NN} vary smoothly as one scans across the region where the FSI effects occur. Nonetheless, our FSI approximation procedure predicts observable effects in *some* of the spin-spin correlation parameters, and, as a test of the model, it would be of interest to see if they are really there experimentally.

We begin by reviewing the standard procedure[7] for including FSI, which consists of multiplying the scattering amplitude by a factor $J^{-1}(p)$. Here $J^{-1}(p)$ is the inverse Jost function for the appropriate partial wave, while p is the relative momentum of the pair of particles under consideration. The Jost function depends on the potential for the interacting pair.[7]

Since the relevant two-nucleon interaction is at low relative energy, we include FSI only if the final pair is in a $^1S_0$ or $^3S_1$ state. The potential is assumed to be given by a separable Yamaguchi form

$$\langle p|V|p'\rangle = -\frac{\lambda}{M}\frac{1}{p^2+\beta^2}\frac{1}{p'^2+\beta^2} \ , \tag{1}$$

which describes low-energy NN scattering very well.[9] For $^1S_0$ the parameters adopted by Yamaguchi are $\lambda_s = 2.22 \times 10^6$ MeV^3 and $\beta_s = 285$ MeV, corresponding to a scattering length $a_s = -23.69$ fm and an effective range, $r_s = 2.158$ fm. For $^3S_1$ the corresponding values are $\lambda_t = 3.16 \times 10^6$ MeV^3, $\beta_t = 285$ MeV, $a_t = 5.378$ fm, and $r_t = 1.72$ fm, respectively. (Since the effective range for the singlet NN system is now better known than when Yamaguchi originally obtained his values, we have also considered parameters $\lambda_s = 1.07 \times 10^6$

MeV^3 and $\beta_s = 225$ MeV which correspond to $a_s = -23.69$ fm and $r_s = 2.76$ fm.)

The advantage of the Yamaguchi form is that the $L = 0$ Jost function can be written down explicitly as

$$J_0(p) = \frac{[1 + 2p^2 |f_0(p)|^2]^{1/2}}{1 + (\beta + ip) f_0(p)} .$$ (2)

Here $f_0(p)$ is the s-wave scattering amplitude, given by

$$f_0(p) = \left[\frac{(\beta^2 + p^2)^2}{2\pi^2 \lambda} + \frac{\beta^2 + p^2}{2\beta} - \beta - ip \right]^{-1} .$$ (3)

The above Jost function has the required property that for large p, $J_0(p) \simeq 1$.

Since the Jost function is only required at low relative energy, it is tempting to use, as many authors do, a "scattering length approximation" in Eq. (2). We know of at least two such approximations, one which takes $f_0 = -a$ and the second which takes $f_0(p) = (-1/a - ip)^{-1}$. We find, however, that both approximations for the Jost function are inadequate for our purposes. The first, which does not satisfy the requirement[7] that the phase of the Jost function be minus that of the scattering amplitude, is poor, both for the absolute value and for the phase, even for small momenta. The second is accurate at extremely small p but begins to deviate noticeably from the exact form by $p \sim 20$ MeV/c. Therefore, in what follows we shall use only the complete form of $J_0(p)$ given by Eqs. (2) and (3).

Finally, we point out why it is necessary to take into account both the $^1S_0$ and $^3S_1$ FSI's described by $J_s^{-1}(p)$ and $J_t^{-1}(p)$, respectively. At low energy the inverse Jost function for the spin singlet is much larger than for the triplet. Also, $J_s^{-1}(p)$ is much more sharply peaked than $J_t^{-1}(p)$. Therefore, the $^1S_0$ FSI tends to be the dominant feature in most reactions. However, in pion production there are some special selection rules due to the odd parity of the pion. The $^1S_0$ state for the final nucleon pair only occurs in the NN$\rightarrow$ NNπ amplitudes with $J = L \pm 1$ initial NN partial

waves. Since most of the pion production occurs in $J = L$ partial waves (14 mb out of 17 mb at 800 MeV),[10] a major part of the FSI effect is due to the $^3S_1$ interaction, and the peaks are relatively wide. We will return, in the discussion below, to the question of an interesting competition between the $^1S_0$ and $^3S_1$ contributions in a typical spin observable near the FSI peak.

Results using the above FSI prescription to modify our three-body model calculations[6] are shown for fully exclusive spin-averaged pp$\rightarrow$ npπ^+ differential cross sections at 800 MeV in Figs. 1–3. These are for three sets of angle pairs (in coplanar geometry with proton and pion on opposite sides of the beam)—($\theta_p = 19°$, $\theta_\pi = 53°$), ($\theta_p = 14.5°$, $\theta_\pi = 42°$), and ($\theta_p = 15°$, $\theta_\pi = 21°$)—where FSI peaks show up strongly. A reasonable fit to the data for the first angle pair is obtained with the FSI prescription exactly as presented above. The results shown in Figs. 2 and 3, however, have both the singlet and triplet inverse Jost functions renormalized by factors of 0.50 and 0.57, respectively. In past discussions of FSI effects, the normalization factor has been treated as a free parameter, presumably dependent on final-state configuration. This introduction of a parameter[11] is based on the belief that the approximation procedure is capable of predicting the shape of the peak correctly, but not necessarily the height. From Figs. 2 and 3 it is clear that this normalization parameter is indeed required and is different in different parts of phase space. Figure 3 also compares our (one-parameter) predictions with those of VerWest's peripheral model calculation.[5]
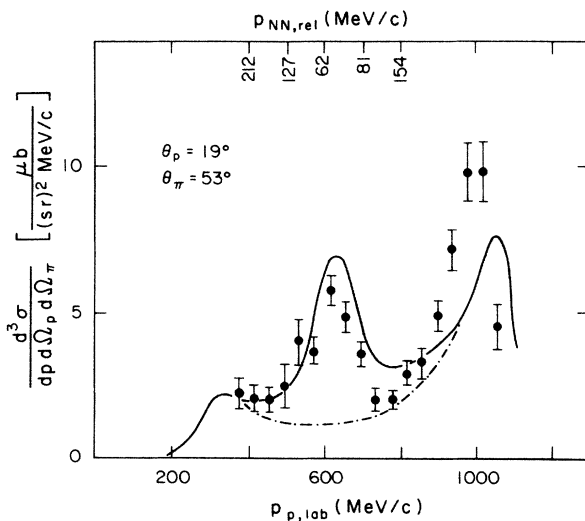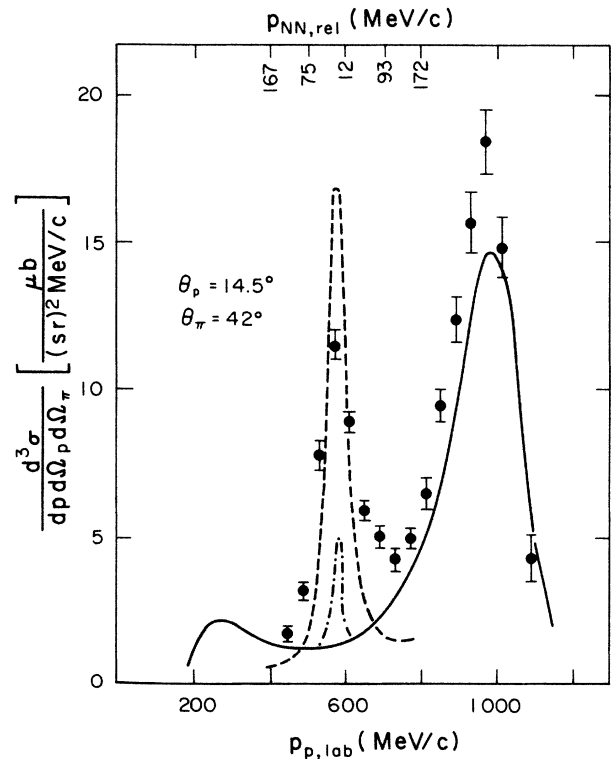

FIG. 1. Proton spectrum for pp$\rightarrow$ pπ^+n at 800 MeV with proton emerging at 19° and pion at 53°. The dashed-dotted curve is the prediction of the three-body model of Ref. 6, while the solid curve shows the effect of the FSI correction (normalization factor = 1). Data are from Ref. 2.

FIG. 2. Proton spectrum for pp$\rightarrow$ pπ^+n at 800 MeV with $\theta_p = 14.5°$ and $\theta_\pi = 42°$. Solid curve is the uncorrected model prediction, and dashed curve shows the FSI correction (with both singlet and triplet Jost function FSI factors renormalized by 0.50). The effect of the $^1S_0$ FSI alone is shown as the dashed-dotted curve. Data are from Ref. 2.
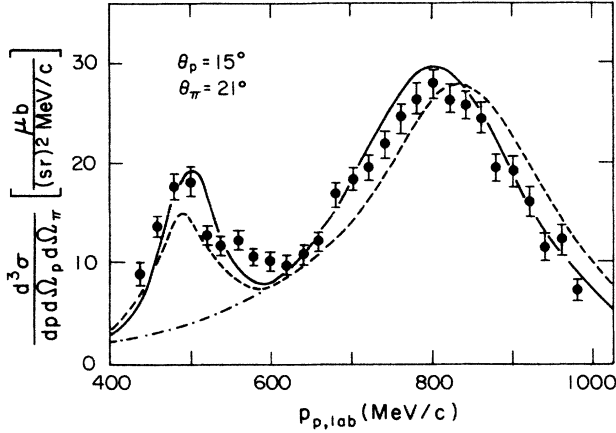
FIG. 3. Proton spectrum for $pp \to p\pi^+ n$ at 800 MeV with $\theta_p = 15°$ and $\theta_\pi = 21°$. Solid curve is full calculation with normalization factor 0.57, and the dashed-dotted curve shows model predictions before FSI corrections. The dashed curve comes from VerWest's model, Ref. 5. Data are from Ref. 1.

The FSI corrections here have been calculated for relative NN momenta up to $p_{max} = 200$ MeV/c, corresponding to a nucleon kinetic energy of 21.3 MeV in the NN rest frame. The width of the FSI peak in Fig. 1 is about 90 MeV/c in momentum, while in Fig. 2 it is about 20 MeV/c. It is hard to estimate the experimental width of very narrow peaks be-
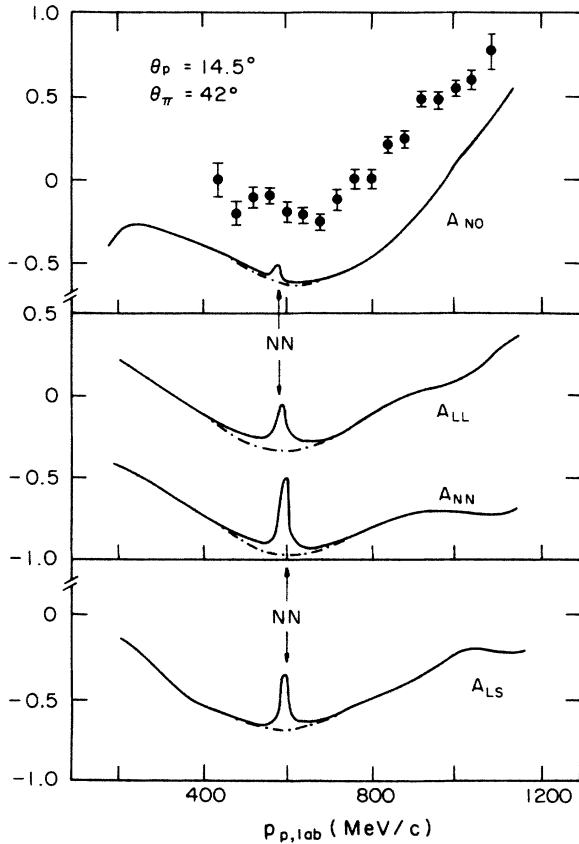
cause of the sparseness of the data points and the low resolution. Furthermore, the smearing of the detector acceptances ought to be considered to make a fair comparison between theory and experiment. At all three angle pairs the FSI peak is mainly due to the $^3S_1$ interaction. The $^1S_0$ contribution alone is shown by the small peak in Fig. 2 (dashed-dotted curve). In the other cases the $^1S_0$ peak would be even smaller. The reason for this is the selection rule, discussed above, which suppresses the $^1S_0$ NN final state. It is also because of this suppression that the predictions of the solid curves are essentially unchanged if we calculate using the alternative set of singlet potential parameters that give the better value of singlet effective range.

It is at this point interesting to see what the effects of FSI are on spin observables. Because one deals with ratios of cross sections here, any question of the normalization of the Jost function is less important than for cross sections. However, the phases of the Jost functions are now crucial. The FSI effects in most spin observables are generally small. They are most pronounced in cases when the cross section peak is very narrow. Figure 4 shows selected results of our calculations for such a case, viz., 800 MeV and ($\theta_p = 14.5°$, $\theta_\pi = 42°$). There are intriguing 40% spikes in the spin-spin correlations, A_{NN}, A_{LL}, and A_{LS}, in the region of lowest relative momentum, while the beam polarization asymmetry A_{N0} shows little effect.

These spikes are caused by a delicate interplay between amplitudes which are enhanced (differently) by the singlet and triplet FSI's. We show the situation for A_{NN} in more detail in Fig. 5, where the $^1S_0$ and $^3S_1$ FSI contributions are

FIG. 4. Selected spin observables as a function of final proton momentum for $pp \to p\pi^+ n$ at 800 MeV, $\theta_p = 14.5°$ and $\theta_\pi = 42°$. Solid curves include FSI correction; dashed-dotted curves do not. Beam polarization asymmetry data are from Ref. 2.
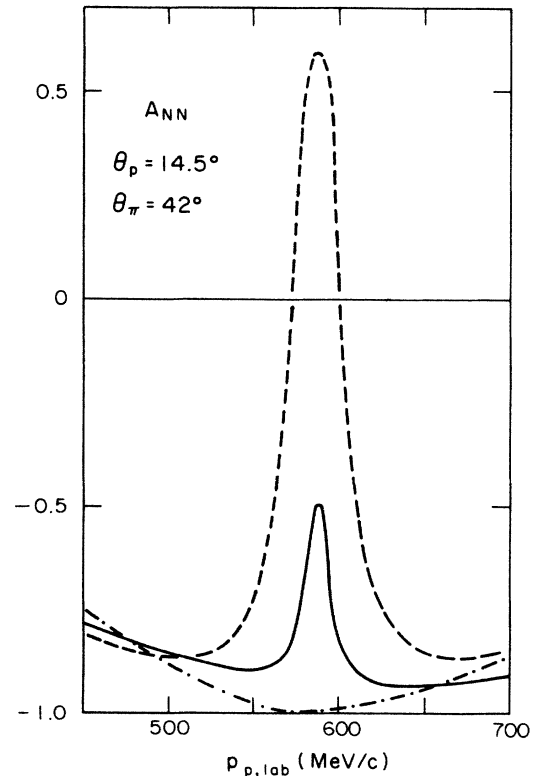

FIG. 5. Spin-spin correlation parameter A_{NN} for same kinematics as in Fig. 4. Solid curve shows the full calculation (same as in Fig. 4). Calculations with only the $^1S_0$ ($^3S_1$) FSI are shown by the dashed (dashed-dotted) curve.

plotted separately. The big effect seen for the $^1S_0$ FSI alone is due to the enhancement of the $J = L \pm 1$ waves. The $^3S_1$ FSI effect alone gives A_{NN} very close to -1 (A_{NN} would be exactly -1 if only singlet initial states were present). When both FSI's are present, the large $^1S_0$ peak is reduced to the smaller spike shown already in Fig. 4.

Clearly, this prediction depends on our assumption that the $^1S_0$ and $^3S_1$ FSI factors are each renormalized by the same amount.[11] Nonetheless, the effects depicted here may be large enough to be seen in experiments employing present state-of-the-art accuracy. The only FSI effect seen experimentally so far in a spin observable is, as far as we know, the reduction of a large negative A_{N0} at low NN invariant masses at beam energies around 500 MeV.[3] We are unfortunately unable to compare calculations directly with the inclusive data shown in Fig. 14 of Ref. 3, since this would involve an integration over the phase space acceptance of the experiment (and this is unknown to us). The FSI-corrected A_{N0} for the case of exclusive final-state geometry shown in Fig. 2 of Ref. 3 is very similar to the curve representing our model predictions without FSI. Unfortunately, the errors on the data do not allow a decision as to whether the predicted FSI effects are actually present.

Finally, we remark that very recent work on spin transfer coefficients[4] shows large FSI peaks in the pion production

cross sections, but there is no apparent FSI structure in the observables D_{NN}, $D_{S\Omega}$, and $D_{L\Omega}$. Here, e.g., $D_{S\Omega} = D_{SS}\cos\Omega + D_{SL}\sin\Omega$, where Ω is the angle of precession of the spin induced by the spectrometer magnet which analyzes the final proton. Our calculations at the relevant kinematics show that D_{SS}, D_{SL}, etc., change appreciably when FSI's are introduced, but the particular combinations $D_{S\Omega}$ and $D_{L\Omega}$ do not.

In conclusion, we have shown that, following a conventional prescription for including final-state interactions, a considerable improvement in our three-body model predictions is obtained in those kinematic situations where the final NN pair has small relative energy. It is mostly in the exclusive differential cross sections that the FSI effects are large. In general, FSI effects on spin observables are small. Here, the dynamically suppressed $^1S_0$ FSI, which would show up dramatically if it stood alone, has its effects cut down substantially because of competition with the $^3S_1$ FSI. It would be interesting to see if effects of this size are, in fact, present in the NN $\rightarrow$ NNπ reaction.

[1]J. Hudomalj-Gabitsch et al., Phys. Rev. C **18**, 2666 (1978).

[2]A. D. Hancock et al., Phys. Rev. C **27**, 2742 (1983).

[3]C. E. Waltham et al., Nucl. Phys. **A433**, 649 (1985).

[4]C. L. Hollas et al., Phys. Rev. Lett. **55**, 29 (1985).

[5]B. J. VerWest, Phys. Lett. **83B**, 161 (1979).

[6]W. M. Kloet and R. R. Silbar, Nucl. Phys. **A338**, 281 (1980); J. Dubach et al., Phys. Lett. **106B**, 29 (1981); J. Phys. G **8**, 475 (1982).

[7]J. R. Taylor, Scattering Theory (Wiley, New York, 1972), pp. 424–432.

[8]D. Ashery et al., Phys. Rev. Lett. **47**, 895 (1981).

[9]Y. Yamaguchi, Phys. Rev. **95**, 1628 (1954). Another separable model for the NN s-wave interaction which could have been used is that of M. Bander [Phys. Rev. **138**, B322 (1964)].

[10]W. M. Kloet and R. R. Silbar, Nucl. Phys. **A364**, 346 (1981).

[11]In principle, the $^1S_0$ and $^3S_1$ inverse Jost functions could be separately normalized, but for simplicity we choose equal normalization factors.